Extrusion of a Beam from a Rotating Base

Arun K. Banerjee*
Lockheed Missiles & Space Company, Sunnyvale, California
and
Thomas R. Kane†
Stanford University, Stanford, California

This paper deals with a new method for simulating motions of a beam that is being extruded from, or retracted into, a rigid body rotating in a general manner. In essence, the method consists of modeling the beam as a series of elastically connected rigid links and then working with equations of motion linearized in the modal coordinates for the links outside the rigid body at a given time. The theory is applied to a problem of current interest, the extrusion/retraction of the WISP antenna from the Shuttle. Simulation results show that beam tip deflections are highly sensitive to the total time devoted to extrusion/retraction, with retraction the less stable process of the two; and the nature of the angular velocity of the rigid body from/into which the beam is being extruded/retracted is found to affect beam behavior significantly.

I. Introduction

CURRENT interest in dynamics of extrusion of a beam from a rotating base stems from project WISP (Waves In Space Plasma), which involves extending two booms from the Shuttle, each to a final length of 150 m and having a tubular cross section with a 0.0635-m diam and a 0.00254-m wall thickness, while the Shuttle is rotating at a rate of 1 deg/s. Clearly, it is helpful in a project of this kind to be able to perform simulations leading to results such as those shown in Figs. 1 and 2, the first of which contains time plots of the tip deflection, the root bending moment, and the length of each boom during an extrusion operation, whereas the second deals with the same quantities during retraction. It is the purpose of this paper to provide an algorithm for the performance of such simulations.

In previous attacks[1-5] on the problem under consideration, beams were modeled as continua, and deflections were described by linear combinations of modal functions weighted by time-dependent "generalized coordinates," an approach familiar from the classical vibrations literature. However, whereas the arguments of the classical modal functions are independent, purely spatial variables, those of the modal functions used in Refs. 1–5 are treated as time-dependent spatial variables. The deployment of tethers,[6] plates,[7] and other structures[8] has been treated similarly. Regarding the soundness of this approach as questionable, we adopt a new technique, one that can be applied not only to the title problem but also to the simulation of motions of continua other than beams undergoing extrusion from, or retraction into, moving bases. In what follows, a simulation algorithm is described in sufficient detail to permit a reader to construct a simulation program; numerical results in addition to those plotted in Figs. 1 and 2 are reported and discussed, and the rationale underlying the algorithm is explained.

II. Algorithm

The algorithm to be described applies to system S (see Fig. 3) that is substituted for an actual system comprising a rigid body and a continuous boom having a linear mass density ρ, principal flexural rigidities EI and EJ, and a varying length. At any given time t, S consists of a rigid body B, one of whose points, O, is fixed in a Newtonian reference frame N; rigid, massless link elements E_i $(i=1,\ldots,n+1)$, each of length L, connected to each other by ball-and-socket joints; particles P_i of masses m_i $(i=1,\ldots,n+2)$ situated at the ends of the links; and two linear torsion springs at each joint, one of modulus KX_i, the other of modulus KY_i $(i=1,\ldots,n)$. The numbering scheme is shown in Fig. 3, which applies to an instant at which m_{n+2} is inside body B. The masses $m_1,\ldots,m_{n+2}$ have the values

$$m_1 = m_{n+2} = \frac{\rho L}{2(n+1)L} \tag{1}$$

$$m_i = \frac{\rho L}{(n+1)L} \qquad (i=2,\ldots,n+1) \tag{2}$$

and the spring moduli are given by

$$KX_i = \frac{EI}{L}, \qquad KY_i = \frac{EJ}{L} \qquad (i=1,\ldots,n-2) \tag{3}$$

$$KX_{n-1} = \frac{6(n-1)EI}{(3n-8)L}, \qquad KY_{n-1} = \frac{6(n-1)EJ}{(3n-8)L} \tag{4}$$

$$KX_n = \frac{3nEI}{2(3n+1)L}, \qquad KY_n = \frac{3nEJ}{2(3n+1)L} \tag{5}$$

An extrusion/retraction process is modeled by treating the integer n as a discontinuous function of time t, prescribing the distance from O to P_{n+1} as a function $d(t)$, and requiring that E_{n+1} remain on a line fixed in B and passing through O. To characterize beam displacements, we introduce a dextral set of mutually perpendicular unit vectors $\boldsymbol{b}_1, \boldsymbol{b}_2, \boldsymbol{b}_3$ fixed in B, with $\boldsymbol{b}_3$ pointing from O to P_{n+1}, let $\boldsymbol{r}^{OP_k}$ be the position vector from O to P_k, and define x_k and y_k as

$$x_k = \boldsymbol{r}^{OP_k} \cdot \boldsymbol{b}_1, \qquad y_k = \boldsymbol{r}^{OP_k} \cdot \boldsymbol{b}_2 \qquad (k=1,\ldots,n) \tag{6}$$

Finally, to deal with the rotational motion of B in N, we specify functions $\omega_1(t), \omega_2(t), \omega_3(t)$ such that the angular velocity of B in N is given by

$${}^N\boldsymbol{\omega}^B = \omega_1 \boldsymbol{b}_1 + \omega_2 \boldsymbol{b}_2 + \omega_3 \boldsymbol{b}_3 \tag{7}$$

The principal purpose of the algorithm is the determination of x_k and y_k $(k=1,\ldots,n)$ as functions of t. This is accomplished by expressing x_k and y_k as

$$x_k = \sum_{j=1}^{\nu} A_{kj} q_j \qquad (k=1,\ldots,n) \tag{8}$$

Received July 13, 1987; revision received Oct. 19, 1987.

*Senior Staff Engineer.
†Professor of Applied Mechanics.

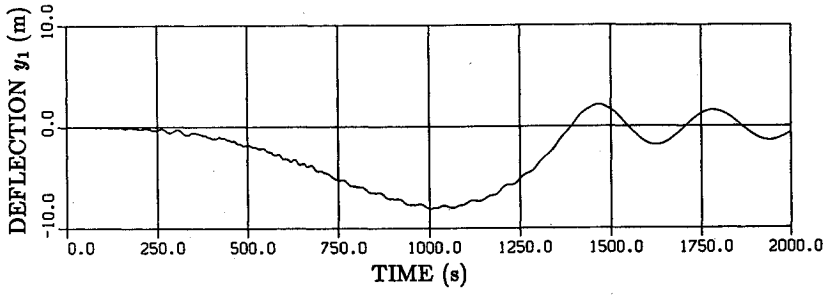

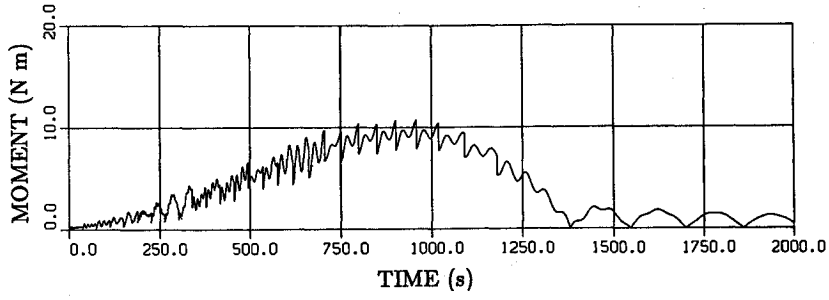

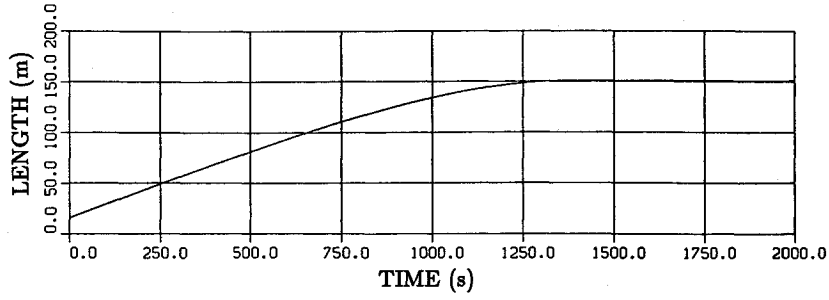

Fig. 1 Extrusion from 15–150 m; angular velocity of base perpendicular to extrusion direction.

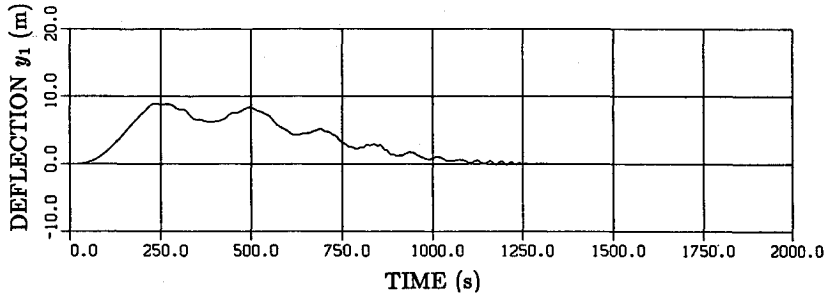

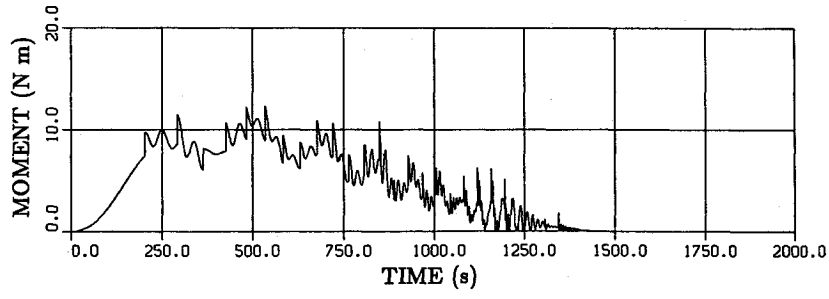

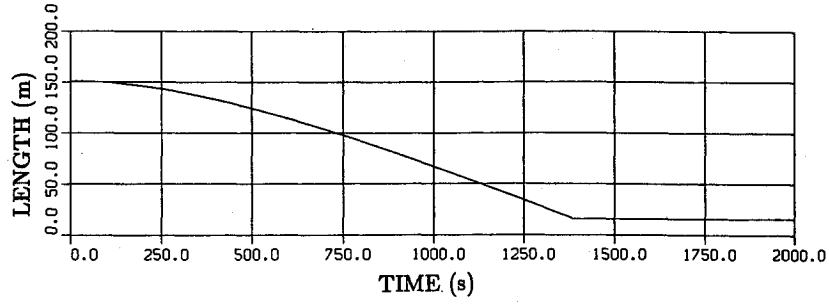

Fig. 2 Retraction from 150–15 m; angular velocity of base perpendicular to retraction direction.

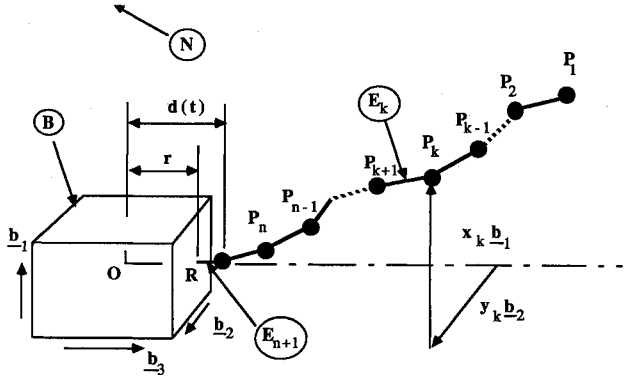

Fig. 3 Substitute system.

$$y_k = \sum_{j=1}^{\nu} B_{kj} q_j \qquad (k = 1, \ldots, n) \tag{9}$$

where ν is an integer selected arbitrarily; A_{kj} and B_{kj} are constants found by performing certain modal analyses; and q_j $(j = 1, \ldots, \nu)$ are time-dependent functions found by numerically integrating a certain set of differential equations. To these ends, one proceeds as follows:

1) Consider the classical small vibrations problem that presents itself when $\omega_1(t)$, $\omega_2(t)$, and $\omega_3(t)$ are equal to zero and $d(t)$ is equal to a constant such that P_{n+1} is outside the physical confines of B. Letting n^* be the largest value of n that will be of interest, determine, for $n = 1, \ldots, n^*$, the natural frequencies Ω_i $(i = 1, \ldots, \nu)$ and the modal matrix normalized with respect to the mass matrix; then, let A_{kj} and B_{kj} $(k = 1, \ldots, n;\ j = 1, \ldots, \nu)$ be those elements of the modal matrix associated with x_k and y_k, respectively.

2) For $n = 1, \ldots, n^*$, form the following modal sums:

$$A_i \triangleq \sum_{k=1}^{n} m_k A_{ki} \qquad (i = 1, \ldots, \nu) \tag{10}$$

$$B_i \triangleq \sum_{k=1}^{n} m_k B_{ki} \qquad (i = 1, \ldots, \nu) \tag{11}$$

$$R_{ij} \triangleq \sum_{k=1}^{n} m_k A_{ki} A_{kj} \qquad (i, j = 1, \ldots, \nu) \tag{12}$$

$$S_{ij} \triangleq \sum_{k=1}^{n} m_k B_{ki} B_{kj} \qquad (i, j = 1, \ldots, \nu) \tag{13}$$

$$T_{ij} \triangleq \sum_{k=1}^{n} m_k \left(B_{ki} A_{kj} - A_{ki} B_{kj} \right) \qquad (i, j = 1, \ldots, \nu) \tag{14}$$

$$U_{ij} \triangleq \sum_{k=1}^{n} m_k \left(A_{ki} B_{kj} + B_{ki} A_{kj} \right) \qquad (i, j = 1, \ldots, \nu) \tag{15}$$

$$C_{kij} \triangleq \sum_{l=k}^{n} L \left[\left(\frac{A_{li} - A_{l+1,i}}{L} \right) \left(\frac{A_{lj} - A_{l+1,j}}{L} \right) + \left(\frac{B_{li} - B_{l+1,i}}{L} \right) \left(\frac{B_{lj} - B_{l+1,j}}{L} \right) \right] \qquad (k = 1, \ldots, n;\ i, j = 1, \ldots, \nu) \tag{16}$$

$$E_{ij} \triangleq \sum_{k=1}^{n} m_k C_{kij} \qquad (i, j = 1, \ldots, \nu) \tag{17}$$

3) For $n = 1, \ldots, n^*$, evaluate the following:

$$G_{ij} \triangleq 2\omega_3 T_{ij} \qquad (i, j = 1, \ldots, \nu) \tag{18}$$

$$K_{ij} \triangleq \dot{\omega}_3 T_{ij} + \omega_1 \omega_2 U_{ij} - \left(\omega_2^2 + \omega_3^2 \right) R_{ij} - \left(\omega_3^2 + \omega_1^2 \right) S_{ij} + \left(\omega_1^2 + \omega_2^2 \right) \sum_{k=1}^{n} m_k C_{kij} \left[d + (n - k + 1) L \right] - \ddot{d} E_{ij} \qquad (i, j = 1, \ldots, \nu) \tag{19}$$

$$f_i \triangleq -\Big\{ \left(\dot{\omega}_2 + \omega_3 \omega_1 \right) \sum_{k=1}^{n} m_k A_{ki} \left[d + (n - k + 1) L \right] - \left(\dot{\omega}_1 - \omega_2 \omega_3 \right) \sum_{k=1}^{n} m_k B_{ki} \left[d + (n - k + 1) L \right] + 2\dot{d} \left(\omega_2 A_i - \omega_1 B_i \right) \Big\} \qquad (i = 1, \ldots, \nu) \tag{20}$$

4) For $n = 1, \ldots, n^*$, form ϕ_n, δ_n, v_n, $q(0)$, and $\dot{q}(0)$ as

$$\phi_n \triangleq \begin{bmatrix} A_{11} & A_{12} & \cdots & A_{1\nu} \\ \cdot & \cdot & \cdots & \cdot \\ \cdot & \cdot & \cdots & \cdot \\ \cdot & \cdot & \cdots & \cdot \\ A_{n1} & A_{n2} & \cdots & A_{n\nu} \\ B_{11} & B_{12} & \cdots & B_{1\nu} \\ \cdot & \cdot & \cdots & \cdot \\ \cdot & \cdot & \cdots & \cdot \\ \cdot & \cdot & \cdots & \cdot \\ B_{n1} & B_{n2} & \cdots & B_{n\nu} \end{bmatrix}, \quad \delta_n \triangleq \begin{bmatrix} x_1(0) \\ \cdot \\ \cdot \\ x_n(0) \\ y_i(0) \\ \cdot \\ \cdot \\ y_n(0) \end{bmatrix},$$

$$v_n \triangleq \begin{bmatrix} \dot{x}(0) \\ \cdot \\ \cdot \\ \dot{x}_n(0) \\ \dot{y}_1(0) \\ \cdot \\ \cdot \\ \dot{y}_n(0) \end{bmatrix} \tag{21}$$

$$q(0) \triangleq \left(\phi_n^T \phi_n \right)^{-1} \phi_n^T \delta_n \tag{22}$$

$$\dot{q}(0) \triangleq \left(\phi_n^T \phi_n \right)^{-1} \phi_n^T v_n \tag{23}$$

5) Find $q_i(0)$ and $\dot{q}_i(0)$ $(i = 1, \ldots, \nu)$ such that

$$\left[q_1(0) \ldots q_\nu(0) \right]^T = q(0) \tag{24}$$

$$\left[\dot{q}_1(0) \ldots \dot{q}_\nu(0) \right]^T = \dot{q}(0) \tag{25}$$

6) After assigning values to the modal damping factors ζ_i $(i = 1, \ldots, \nu)$ and using the initial values found in step 5, perform a numerical integration of the differential equations

$$\ddot{q}_i + \sum_{j=1}^{\nu} \left[G_{ij} \dot{q}_j + K_{ij} q_j \right] + 2\zeta_i \Omega_i \dot{q}_i + \Omega_i^2 q_i = f_i \qquad (i = 1, \ldots, \nu) \tag{26}$$

throughout the time interval $t_0 \le t \le T + t_0$, with T such that

$$L = \int_{t_0}^{t_0 + T} \dot{d}(t)\, \mathrm{d}t \tag{27}$$

where t_0 is zero at the beginning of extrusion. If $n < n^*$ when n links have been extruded, replace n with $n + 1$ in Eqs. (21–23), assigning to $x_i(0)$, $y_i(0)$, $\dot{x}_i(0)$, $\dot{y}_i(0)$ $(i = 1, \ldots, n)$ the

terminal values from the preceding stage of the extrusion while setting $x_{n+1}, y_{n+1}, \dot{x}_{n+1}, \dot{y}_{n+1}$ equal to zero. To simulate retraction of the beam, simply reverse this procedure.

7) To find the deflection of the beam tip, evaluate x_1 and y_1 as

$$x_1 = \sum_{j=1}^{\nu} A_{1j} q_j \tag{28}$$

$$y_1 = \sum_{j=1}^{\nu} B_{1j} q_j \tag{29}$$

8) The dynamic bending moment at the root R of the beam is given by

$$M = \sqrt{M_1^2 + M_2^2} \tag{30}$$

where, if r denotes the distance OR in Fig. 3,

$$\begin{aligned} M_1 = &- \sum_{k=1}^{n} m_k [d - r + (n-k+1)L] \\ &\times \Bigg\{ (\dot{\omega}_3 + \omega_1\omega_2) \sum_{j=1}^{\nu} A_{kj} q_j \\ &- (\omega_1^2 + \omega_3^2) \sum_{j=1}^{\nu} B_{kj} q_j + 2\omega_3 \sum_{j=1}^{\nu} A_{kj} \dot{q}_j \\ &+ \sum_{j=1}^{\nu} B_{kj} \ddot{q}_j - 2\omega_1 \dot{d} - (\dot{\omega}_1 - \omega_2\omega_3)[d + (n-k+1)L] \Bigg\} \\ &- \sum_{k=1}^{n} m_k \{ (\omega_1^2 + \omega_2^2)[d + (n-k+1)L] - \ddot{d} \} \sum_{j=1}^{\nu} B_{kj} q_j \end{aligned} \tag{31}$$

$$\begin{aligned} M_2 = &\sum_{k=1}^{n} m_k [d - r + (n-k+1)L] \\ &\times \Bigg\{ (-\dot{\omega}_3 - \omega_1\omega_2) \sum_{j=1}^{\nu} B_{kj} q_j \\ &- (\omega_2^2 + \omega_3^2) \sum_{j=1}^{\nu} A_{kj} q_j - 2\omega_3 \sum_{j=1}^{\nu} B_{kj} \dot{q}_j \\ &+ \sum_{j=1}^{\nu} A_{kj} \ddot{q}_j + 2\omega_2 \dot{d} + (\dot{\omega}_2 + \omega_3\omega_1)[d + (n-k+1)L] \Bigg\} \\ &+ \sum_{k=1}^{n} m_k \{ (\omega_1^2 + \omega_2^2)[d + (n-k+1)L] - \ddot{d} \} \sum_{j=1}^{\nu} A_{kj} q_j \end{aligned} \tag{32}$$

III. Simulations

The algorithm set forth in Sec. II was programmed to simulate extrusions/retractions of a WISP antenna from a slowly rolling Shuttle. The antenna is a tube having a 0.0635-m diameter, a 0.00254-m wall thickness, a mass density of 0.3644 kg/m, and a Young's modulus of 1.96491×10^{11} N/m^2, and exhibiting material damping of 5–9%. Fully deployed, the antenna is 150 m long.

To test the computer program, as well as the soundness of the underlying modeling method, we first consider a problem for which results can be obtained by means of an available continuum theory,[9] namely, the problem of simulating motions of the fully deployed boom during a "spin-up" maneuver such that $\omega_2 = \omega_3 = 0$ while

$$\omega_1(t) = \frac{0.125}{57.3 \times 300} \left[t - \frac{150}{\pi} \sin \frac{\pi t}{150} \right] \text{ rad/s}, \quad t \le 300 \text{ s} \tag{33}$$

and $\omega_1 = 0.0021815$ for $t > 300$ s. When rotatory inertia is neglected and 5% modal damping is included, the aforementioned continuum theory leads to tip deflection y_1 vs time t plot shown as a solid curve in Fig. 4. The corresponding results obtained by using the present theory with L equal to 5 m and $n^* = 29$ are plotted as a dashed curve in Fig. 4. As can be seen, the two curves agree very well; and the agreement is found to improve when the number of elements used to represent the boom is increased. Moreover, this example demonstrates that the theory at hand captures the phenomenon of "centrifugal stiffening," which plays an important role in connection with problems of the kind under consideration. Finally, it is worth noting that the spin-up problem is of interest in its own right, for it highlights the considerable sensitivity of beam deflections to "rise" time, that is, the time devoted to bringing the angular speed of the Shuttle to a desired final value.

The results reported in Figs. 1 and 2 apply to extrusion/retraction maneuvers during which the Shuttle rotates at a steady rate of 1 deg/s about an axis normal to the direction of extrusion/retraction. Extrusion from 15 to 150 m and retraction from 150 to 15 m are completed in 1387 s when the extrusion rate is prescribed as

$$\dot{d} = v_{\max} \left[1 - \left(\frac{t}{T_{\max}} \right)^3 \right] \tag{34}$$

while the retraction rate is specified as

$$\dot{d} = -v_{\max} \left[1 - \left(\frac{T_{\max} - t}{T_{\max}} \right)^3 \right] \tag{35}$$

with $v_{\max} = 0.133$ m/s and $T_{\max} = 1500$ s. These extrusion/retraction profiles have the merit of simplicity, but they are somewhat unrealistic because they involve an inappropriately abrupt initiation/termination of the extrusion/retraction process. Two modes are used to characterize bending in each principal plane, that is, $\nu = 4$, and 5% modal damping is introduced by letting $\zeta_1 = \zeta_2 = 0.05$. The allowable bending moment for this beam is equal to 135 N-m.

As long as the angular velocity of the base B is perpendicular to $\boldsymbol{b}_3$, the extrusion/retraction direction, beam deflections occur only in the plane perpendicular to the angular velocity vector and can be attributed to the Coriolis effect. Thus, their magnitude may be expected to be proportional both to the base spin rate and the extrusion/retraction speed, and additional computer runs confirm this expectation; it is worth noting that tip deflections can easily become quite large, particularly during retraction, approaching the limit of applicability of linear elasticity theory.

The algorithm at hand also accommodates base motions more general than the one just considered. In particular, it applies when the angular velocity of B in N has a relatively large component perpendicular to the direction of extrusion/retraction, and a relatively small component in this direction, the latter component being present as the result of, say, a malfunction in the control system governing the attitude motions of B. To form an idea of the extent to which deflections and moments encountered under these circumstances differ from those found previously, we set

$$\omega_1 = \left(\frac{1}{1.01} \right)^{1/2} \text{ deg/s}, \qquad \omega_2 = 0, \qquad \omega_3 = 0.1\omega_1 \tag{36}$$

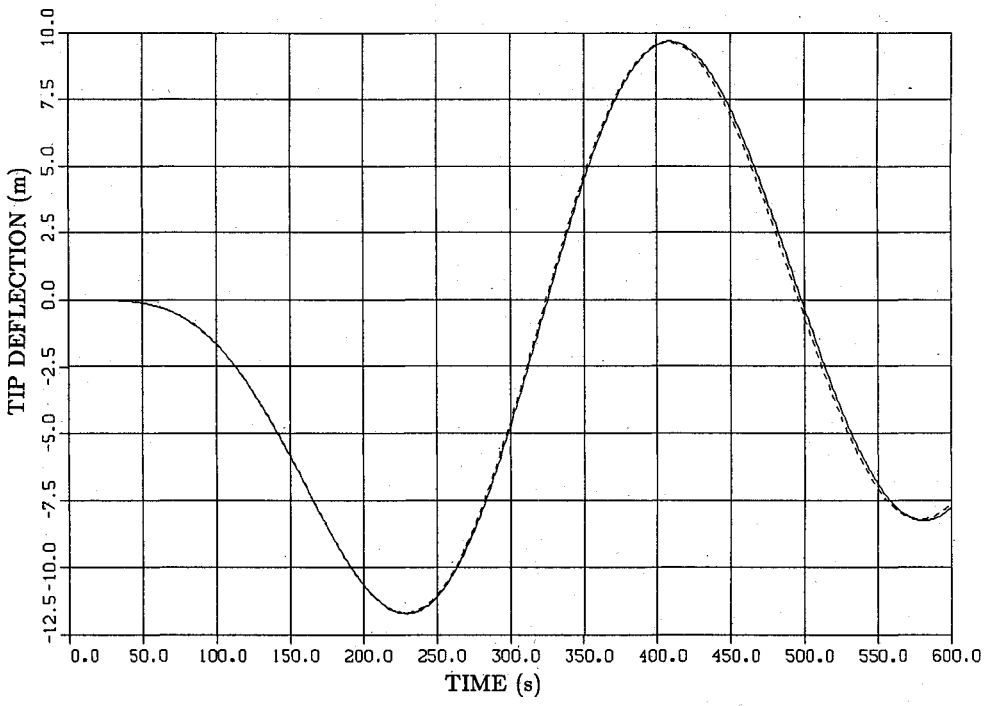

Fig. 4 Spin-up maneuver; comparison of present theory with theory of Ref. 9.

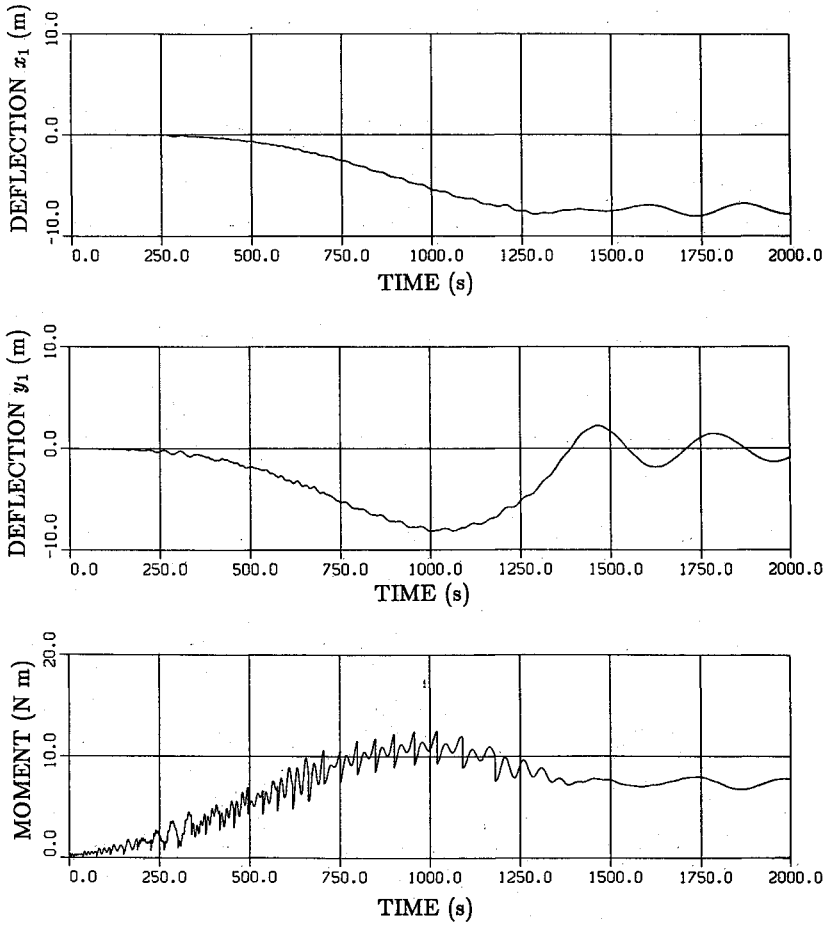

Fig. 5 Extrusion from 15–150 m; angular velocity of base *not* perpendicular to extrusion direction.

so that, as before, the angular velocity of B in N has a magnitude of 1 deg/s. The resulting beam responses during extrusion and retraction are shown in Figs. 5 and 6, respectively. Each of these figures, like Figs. 1 and 2, contains a plot of the tip deflection y_1 and the root bending moment M as a function of time t; in addition, the tip deflection x_1 is plotted as the uppermost curve in Figs. 5 and 6. This deflection, which takes place in a direction parallel to the major component of ${}^N\boldsymbol{\omega}^B$, is of particular interest for two reasons: it occurs only if ${}^N\boldsymbol{\omega}^B$ has a component in the extrusion/retraction direction (which is the reason it was not plotted in Figs. 1 and 2); and it persists subsequent to the completion of an extrusion operation. As for y_1 and M, a comparison of the relevant curves in Figs. 1 and 5, on the one hand, and Figs. 2 and 6, on the other

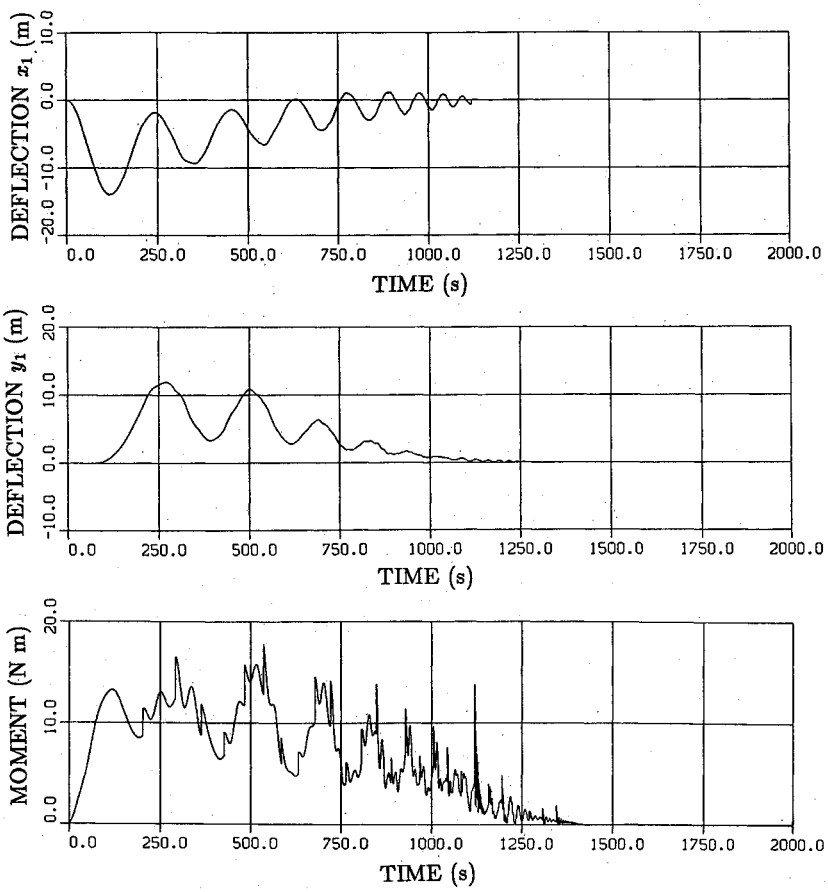

Fig. 6 Retraction from 150–15 m; angular velocity of base *not* perpendicular to retraction direction.

hand, indicates that the presence of a small component of ${}^N\boldsymbol{\omega}^B$ in the extrusion/retraction direction has relatively little effect on y_1 but alters M noticeably, particularly during extrusion, where it not only causes M to acquire a larger maximum value but prevents M from vanishing subsequent to the extrusion. In summary, the presence of a small beam-axis component of the base angular velocity is seen to give rise to a potentially objectionable whirl subsequent to the extrusion.

IV. Rationale

After defining J_i as

$$J_i \triangleq 1 - \left(\frac{x_i - x_{i+1}}{L}\right)^2 + \left(\frac{y_i - y_{i+1}}{L}\right)^2 \qquad (i = 1, \ldots, n) \quad (37)$$

one can express the velocity of point P_k in N (see Fig. 3) as

$$\begin{aligned} {}^N\boldsymbol{v}^{P_k} = {}^N\boldsymbol{\omega}^B \times \left[x_k \boldsymbol{b}_1 + y_k \boldsymbol{b}_2 + \left(d + L \sum_{i=k}^{n} J_i^{1/2} \right) \boldsymbol{b}_3 \right] \\ + \dot{x}_k \boldsymbol{b}_1 + \dot{y}_k \boldsymbol{b}_2 + \dot{d} \boldsymbol{b}_3 \\ - L \sum_{i=k}^{n} J_i^{-1/2} \left[\left(\frac{x_i - x_{i+1}}{L} \right) \left(\frac{\dot{x}_i - \dot{x}_{i+1}}{L} \right) \right. \\ \left. + \left(\frac{y_i - y_{i+1}}{L} \right) \left(\frac{\dot{y}_i - \dot{y}_{i+1}}{L} \right) \right] \boldsymbol{b}_3 \qquad (k = 1, \ldots, n) \end{aligned} \quad (38)$$

A reduction in the number of coordinates used to specify the configuration of the system is effected by introducing modal coordinates q_i $(i = 1, \ldots, \nu)$ as in Eqs. (8) and (9). Thereupon, with N_{lij} defined as

$$\begin{aligned} N_{lij} \triangleq \left(\frac{A_{li} - A_{l+1,i}}{L} \right) \left(\frac{A_{lj} - A_{l+1,j}}{L} \right) + \left(\frac{B_{li} - B_{l+1,i}}{L} \right) \\ \times \left(\frac{B_{lj} - B_{l+1,j}}{L} \right) \qquad (l, i, j = 1, \ldots, n) \end{aligned} \quad (39)$$

Equation (38) gives way to

$$\begin{aligned} {}^N\boldsymbol{v}^{P_k} = {}^N\boldsymbol{\omega}^B \times \left\{ \sum_{j=1}^{\nu} \left(A_{kj} \boldsymbol{b}_1 + B_{kj} \boldsymbol{b}_2 \right) q_j + \left[d + L \sum_{i=k}^{n} J_i^{1/2} \right] \boldsymbol{b}_3 \right\} \\ + \sum_{j=1}^{\nu} \left(A_{kj} \boldsymbol{b}_1 + B_{kj} \boldsymbol{b}_2 \right) \dot{q}_j \\ + \left(\dot{d} - L \sum_{l=k}^{n} J_l^{-1/2} \sum_{i=1}^{\nu} \sum_{j=1}^{\nu} N_{lij} \dot{q}_i q_j \right) \boldsymbol{b}_3 \\ (k = 1, \ldots, n) \end{aligned} \quad (40)$$

and the ν partial velocities of P_k in N now can be identified by inspection (see Ref. 10, p. 48) as

$$\begin{aligned} {}^N\boldsymbol{v}_i^{P_k} = A_{ki} \boldsymbol{b}_1 + B_{ki} \boldsymbol{b}_2 - L \sum_{l=k}^{n} \sum_{j=1}^{\nu} J_l^{-1/2} N_{lij} q_j \boldsymbol{b}_3 \\ (k = 1, \ldots, n;\ i = 1, \ldots, \nu) \end{aligned} \quad (41)$$

In conformity with proper linearization procedure (see Ref. 10, p. 171), linearization in q_i and $\dot{q}_i$ $(i = 1, \ldots, \nu)$ can now be undertaken. In the sequel, a tilde placed over a symbol representing a function of q_i and/or $\dot{q}_i$ $(i = 1, \ldots, \nu)$ signifies that the function has been linearized in these quantities. For example, referring to Eqs. (37), (8), and (9), one can verify that

$$\tilde{J}_i = 1 \qquad (i = 1, \ldots, n) \quad (42)$$

and, with the aid of Eqs. (16) and (39), one obtains, for the linearized partial velocity of P_k,

$$\begin{aligned} {}^N\tilde{\boldsymbol{v}}_i^{P_k} = A_{ki} \boldsymbol{b}_1 + B_{ki} \boldsymbol{b}_2 - \sum_{j=1}^{\nu} C_{kij} q_j \boldsymbol{b}_3 \\ (k = 1, \ldots, n;\ i = 1, \ldots, \nu) \end{aligned} \quad (43)$$

while linearization of Eq. (40) leads to

$$
{}^{N}\tilde{\boldsymbol{v}}^{P_k} = {}^{N}\boldsymbol{\omega}^{B} \times \left\{ \sum_{j=1}^{\nu} \left(A_{kj}\boldsymbol{b}_1 + B_{kj}\boldsymbol{b}_2 \right) q_j + [d + L(n-k+1)]\boldsymbol{b}_3 \right\} + \sum_{j=1}^{\nu} \left(A_{kj}\boldsymbol{b}_1 + B_{kj}\boldsymbol{b}_2 \right) \dot{q}_j + \dot{d}\boldsymbol{b}_3 \qquad (k = 1, \ldots, n) \tag{44}
$$

This equation may be differentiated with respect to t in N in order to obtain the linearized acceleration of P_k in N; that is,

$$
{}^{N}\tilde{\boldsymbol{a}}^{P_k} = \frac{{}^{B}d}{\mathrm{d}t}\left({}^{N}\tilde{\boldsymbol{v}}^{P_k}\right) + {}^{N}\boldsymbol{\omega}^{B} \times {}^{N}\tilde{\boldsymbol{v}}^{P_k} \qquad (k = 1, \ldots, n) \tag{45}
$$

where ${}^{N}\boldsymbol{\omega}^{B}$ is given by Eq. (7); and the generalized inertia forces are now formed as

$$
\tilde{F}_i^{*} = -\sum_{k=1}^{n} m_k^{N}\tilde{\boldsymbol{a}}^{P_k} \cdot {}^{N}\tilde{\boldsymbol{v}}_i^{P_k} \qquad (i = 1, \ldots, \nu) \tag{46}
$$

With the aid of Eqs. (10–20), one thus arrives at (recall that the modes were normalized with respect to the mass matrix in the small vibrations problem)

$$
\tilde{F}_i^{*} = -\ddot{q}_i - \sum_{j=1}^{\nu} \left(G_{ij}\dot{q}_j + K_{ij}q_j \right) - f_i \qquad (i = 1, \ldots, \nu) \tag{47}
$$

As is customary in structural dynamics,[11] we express the generalized active forces associated with the springs and assumed modal damping as

$$
\tilde{F}_i = -\Omega_i^2 q_i - 2\zeta_i \Omega_i \dot{q}_i \qquad (i, \ldots, \nu) \tag{48}
$$

where Ω_i is the ith modal frequency and ζ_i the ith assumed modal damping factor. This brings us into position to write the linearized equations of motion of S by substituting from Eqs. (47) and (48) into

$$
\tilde{F}_i + \tilde{F}_i^{*} = 0 \qquad (i = 1, \ldots, \nu) \tag{49}
$$

which leads to Eqs. (26).

Physically meaningful initial conditions are imposed by specifying the initial values of x_i, y_i, $\dot{x}_i$, and $\dot{y}_i$ $(i = 1, \ldots, n)$. The associated initial values of q_j and $\dot{q}_j$ $(j = 1, \ldots, \nu)$ must satisfy conditions that follow directly from Eqs. (8) and (9); and, with the aid of the symbols defined in Eqs. (21), one can express these conditions as

$$
\phi_n q(0) = \delta_n \tag{50}
$$

$$
\phi_n \dot{q}(0) = v_n \tag{51}
$$

whereupon pseudoinversion yields Eqs. (22) and (23). The initial values of q_j and $\dot{q}_j$ $(j = 1, \ldots, \nu)$ are then found by using Eqs. (24) and (25).

Once Eqs. (26) have been solved subject to the initial conditions as stated in Eqs. (24) and (25), displacements are found by substituting into Eqs. (8) and (9). As for $\boldsymbol{M}$, the moment at the root of the beam, this is given by

$$
\boldsymbol{M} = \sum_{k=1}^{n} \boldsymbol{r}^{RP_k} \times \left(m_k^{N}\boldsymbol{a}^{P_k} \right) \tag{52}
$$

where

$$
\boldsymbol{r}^{RP_k} = \sum_{j=1}^{\nu} \left(A_{kj}\boldsymbol{b}_1 + B_{kj}\boldsymbol{b}_2 \right) q_j + [d - r + (n-k+1)L]\boldsymbol{b}_3 \tag{53}
$$

The magnitude M of the root bending moment is found by using Eq. (30) after evaluating M_1 and M_2, defined as

$$
M_i \triangleq \boldsymbol{M} \cdot \boldsymbol{b}_i \qquad (i = 1, 2) \tag{54}
$$

which leads to Eqs. (31) and (32).

V. Conclusion

The modeling approach, equations of motion formulation method, and computation algorithm used here can be adapted readily to the simulation of extrusions/retractions of continua other than beams, such as tethers and plates. However, because the theory involves linearization in the generalized coordinates and their time derivatives, it can be expected to yield useful results only when the continuum under consideration performs motions during which elastic deformations remain relatively small. Simulations for the WISP antenna show that the deformations become excessively large when the extrusion/retraction time is reduced to, for example, 600 s. A theory free from the restriction to small deformations can be constructed by using as generalized speeds the time derivatives of displacements rather than of generalized coordinates and then writing fully nonlinear differential equations of motion. Such a formulation is currently under development.

Acknowledgment

The authors wish to express their gratitude to Mr. Mario Rheinfurth of the Marshall Space Flight Center, Huntsville, Alabama, for supplying information about the WISP antenna project.

References

[1]Cherchas, D.B., "Dynamics of Spin-Stabilized Satellites During Extension of Long Flexible Booms," *Journal of Spacecraft and Rockets*, Vol. 8, July 1971, pp. 802–804.

[2]Lips, K.W. and Modi, V.J., "Three-Dimensional Response Characteristics for Spacecraft with Deploying Flexible Appendages," *Journal of Guidance and Control*, Vol. 4, Nov.–Dec. 1981, pp. 650–656.

[3]Tsuchiya, K., "Dynamics of a Spacecraft During Extension of Flexible Appendages," *Journal of Guidance, Control, and Dynamics*, Vol. 6, March–April 1983, pp. 100–103.

[4]Jankovic, M.S., "Comment on 'Dynamics of a Spacecraft During Extension of Flexible Appendages,'" *Journal of Guidance, Control, and Dynamics*, Vol. 7, Jan.–Feb. 1984, p. 128.

[5]Lips, K.W., Graham, W.B. Vigneron, F.R., and Hunter, D.G., "Dynamics and Control Characteristics for the WISP 300m Dipole Antenna/Shuttle Configuration," AAS Paper 85-365, Aug. 1985.

[6]Misra, A.K. and Modi, V.J., "A General Dynamical Model for the Space Shuttle Based Tethered Subsatellite System," *Advances in the Astronautical Sciences*, Vol. 40, Pt. II, 1979, pp. 537–557.

[7]Ibrahim, A.M. and Misra, A.K., "Attitude Dynamics of a Satellite during Deployment of Large Plate-Type Structures," *Journal of Guidance, Control, and Dynamics*, Vol. 5, Sept.–Oct. 1982, pp. 442–447.

[8]Hughes, P.C., "Deployment Dynamics of the Communications Technology Satellite—A Progress Report," Paper N76-28328, Symposium on the Dynamics and Control of Nonrigid Space Vehicles, Fracati, Italy, May 1976.

[9]Kane, T.R., Ryan, R.R., and Banerjee, A.K., "Dynamics of a Cantilever Beam Attached to a Moving Base," *Journal of Guidance, Control, and Dynamics*, Vol. 10, March–April 1987, pp. 139–151.

[10]Kane, T.R. and Levinson, D.A., *Dynamics: Theory and Applications*, McGraw-Hill, New York, 1985, pp. 48, 171.

[11]Craig, R.R., Jr., *Structural Dynamics*, Wiley, New York, 1981, p. 354.